Journal of Mammalogy, XX(X):1–13, 2019
DOI:10.1093/jmammal/gyz081

Characterizing wing tears in common pipistrelles (*Pipistrellus pipistrellus*): investigating tear distribution, wing strength, and possible causes

Rana Osama S. Khayat, Kirsty J. Shaw, Gary Dougill, Louise M. Melling, Glenn R. Ferris, Glen Cooper, and Robyn A. Grant*

School of Science and the Environment, John Dalton Building, Manchester Metropolitan University, Chester Street, Manchester, M1 5GD, United Kingdom (ROSK, KJS, GD, LMM, RAG)
School of Healthcare Science, John Dalton Building, Manchester Metropolitan University, Chester Street, Manchester, M1 5GD, United Kingdom (GRF)
School of Mechanical, Aerospace and Civil Engineering, George Begg Building, University of Manchester, Manchester, M1 3BB, United Kingdom (GC)

* *Correspondent: robyn.grant@mmu.ac.uk*

Bats have large, thin wings that are particularly susceptible to tearing. Anatomical specializations, such as fiber reinforcement, strengthen the wing and increase its resistance to puncture, and an extensive vasculature system across the wing also promotes healing. We investigated whether tear positioning is associated with anatomy in common pipistrelles (*Pipistrellus pipistrellus*). Wing anatomy was described using histological techniques, imaging, and material testing. Tear information, including type, position, time in rehabilitation, and possible causes, was collected from rehabilitators of injured bats across the United Kingdom. Results suggest that the position of the plagiopatagium (the most proximal wing section to the body), rather than its anatomy, influenced the number, location, and orientation of wing tears. While material testing did not identify the plagiopatagium as being significantly weaker than the chiropatagium (the more distal sections of the wing), the plagiopatagium tended to have the most tears. The position of the tears, close to the body and toward the trailing edge, suggests that they are caused by predator attacks, such as from a cat (*Felis catus*), rather than collisions. Consistent with this, 38% of *P. pipistrellus* individuals had confirmed wing tears caused by cats, with an additional 38% identified by rehabilitators as due to suspected cat attacks. The plagiopatagium had the lowest number of blood vessels and highest amounts of elastin fibers, suggesting that healing may take longer in this section. Further investigations into the causes of tears, and their effect on flight capabilities, will help to improve bat rehabilitation.

Key words: bat wing, collagen, elastin, healing, material testing, plagiopatagium, wing tear

Bats have thin wing membranes well adapted to generate appropriate lift and thrust to be maneuverable during flight (Vaughan 1970; Swartz et al. 1996; Neuweiler 2000). However, the large area and the thin membranous material of the wings make them particularly susceptible to injuries, such as holes and tears (Ceballos-Vasquez et al. 2015). Davis (1968) found over 40% of pallid bats (*Antrozous pallidus*) in one rural roost had wing injuries or abnormalities. While bats can fly with large wing tears (Davis 1968; Voigt 2013), hundreds of bats are taken to rescue centers for rehabilitation annually in the United Kingdom, especially the common pipistrelle, *Pipistrellus pipistrellus* (Kelly et al. 2008). Indeed, 748 *Pipistrellus* spp. were admitted to just one rescue center in the United Kingdom between 1997 and 2006 (Kelly et al. 2008). Tears are considered significant and severe injuries (Molony et al. 2007; Kelly et al. 2008). Rehabilitation in captivity can also result in increased stress (Moorhouse et al. 2007); therefore, the tear and resulting rehabilitation can significantly affect animal health and welfare (Molony et al. 2007; Kelly et al. 2008). Even though several studies have investigated wing tears in bats (Davis 1968; Powers et al. 2013; Voigt 2013; Greville et al. 2018), there is little characterization of their form (position, orientation, size) and what causes them, although collisions (Davis 1968), fungal infections (Reichard and Kunz 2009; Cryan et al. 2010; Fuller

et al. 2011), and predator attacks (Speakman 1991; Woods et al. 2003; Ancillotto et al. 2013; Loss et al. 2013) are all likely.

Urbanization is likely to increase the occurrence of wing tear injuries in bats, due to a greater likelihood of collisions with man-made structures and the increase in abundance of urban predators, such as cats (*Felis catus*). Urbanization is one of the most dramatic forms of land-use change (Lintott et al. 2015) and it is difficult to predict how it will affect individual species (Mehr et al. 2011; Hale et al. 2012; Lintott et al. 2015; Jung and Threlfall 2018; Santini et al. 2019). Many bats, such as *P. pipistrellus*, exploit urban environments (Mendes et al. 2014; Hale et al. 2015), especially for roosting, water, and foraging under lights (Russo and Ancillotto 2015). However, this also exposes them to urban risks, including predation (Woods et al. 2003). For example, in the United Kingdom, domestic cats are the most abundant carnivores (Woods et al. 2003), and their numbers are concentrated around urban areas (Aegerter et al. 2017). Evidence has suggested that cats target house-roosting bats in both rural and semi-urban areas, with repeated predation events having the capacity to wipe out entire roosts (Ancillotto et al. 2013). However, many of these observations are only occasional and not based on strong evidence (Woods et al. 2003; Ancillotto et al. 2013). A better description of wing tears and their causes is needed in order to understand the scale of the problem in the short term, and to develop management practices in the long term, in terms of treatment and rehabilitation practices.

Bat wings can heal from tears (Davis and Doster 1972; Faure et al. 2009; Weaver et al. 2009), and it has been proposed to use fruit bat wings as a model to study wound healing and contraction (Church and Warren 1968). Bat wings also have an extensive blood supply to enable wound cleaning, prevention of infection, and tissue reformation (Faure et al. 2009). Faure et al. (2009) found that the uropatagium (interfemoral membrane) healed faster than the chiropatagium in big brown bats (*Eptesicus fuscus*), and attributed it to increased vasculature in that area. Moreover, while bat wings are thin and susceptible to tearing, anatomical specializations, such as a net-like fiber system containing collagen and elastin, reinforce the wings and increase their resistance to puncture (Studier 1972; Holbrook and Odland 1978; Madej et al. 2012; Cheney et al. 2017). This is especially true in ground-foraging bats, whose wings are more resistant to puncture and less elastic than bats who forage in more open habitats (Studier 1972). The complex anatomy of the wing, including wing fibers and strength, might affect the position and type of wing tears.

We characterized wing tear injuries in the common pipistrelle, and provide a quantitative summary of tear types, distributions, and rehabilitation outcomes. We examined the anatomy of *P. pipistrellus* wings to identify whether wing vasculature, strength, and fiber distribution are associated with the position and type of wing tears. In particular, we investigated vasculature, material properties, fiber type, and fiber orientation. If anatomy influences tearing, we expect 1) more tears to occur in the weakest wing section (based on material property data); 2) tears should not have a specific orientation because net-like fibers should reinforce equally in all orientations; and 3) tears should heal fastest in the section with the most blood vessels, which should transport factors for wound cleaning and new tissue formation. We collected data from bat rehabilitators across the United Kingdom to characterize wing tear injuries, and discuss some likely causes of tears based on first-hand observations. Our results suggest that the position of the plagiopatagium, rather than its anatomy, influenced the number, location, and orientation of wing tears. Predator attacks were the likely cause of many of the tears, and we suggest that predators directing their attacks toward the bat's body caused many of the rostro-caudal tears in the plagiopatagium.

Materials and Methods

We refer to the anatomy of *P. pipistrellus* wings over three sections (Fig. 1a). The most distal section of the chiropatagium (CI) is the membrane between digits iii and iv. The second section of the chiropatagium (CII) is the membrane between digits iv and v. The most proximal section of the wing is the plagiopatagium (P), which is the membrane between digit v and the body. Ethical approval for the study was obtained through the Research Ethics and Governance Committee at Manchester Metropolitan University, and all tissue was held under a Natural England license (2014-4322-SCI-SCI). Methods conformed to guidelines of the American Society of Mammalogists for the use of wild mammals in research (Sikes et al. 2016).

Ten adult whole-animal *P. pipistrellus* specimens from euthanized animals were donated by bat rehabilitators for vessel tracing (two bats, right side wings), and histology (two bats used in Masson's Trichrome staining and two bats used in Verhoeff-Van Gieson [VVG] staining, right side wings) and material testing (10 bats in total, left side wings, including the six bats from the vessel and histology work). These animals were admitted to care following injury and grounding; although exact details were not known by the rehabilitators, they likely had many internal injuries and complications. All individuals had intact wings so we could examine their anatomy. All photography was undertaken from live adult animals during usual husbandry and rehabilitation procedures carried out by bat rehabilitators (eight *P. pipistrellus* bats for vessel tracing, 55 *P. pipistrellus* bats, and 22 other United Kingdom bats for characterization of tears). Bat rehabilitators were trained individuals registered with the Bat Conservation Trust (BCT).

Vessel tracing.—Ten bat specimens were used to identify the major blood vessels in *P. pipistrellus* wings. Two whole-bat euthanized specimens were donated by bat rehabilitators. Their right wings were removed whole and stored in 4% paraformaldehyde (PFA), at 4°C. The wings were stretched out over a bright lightbox (LEDW-BL-100/100-SLLUB-Q-1R24, Phlox, Aix-en-Provence, France), and photographed using a digital camera (D3200, Nikon, Tokyo, Japan; Fig. 1a). Another eight photographs were collected from bat rehabilitators, who had stretched the wings of live bats, admitted for rehabilitation, over a white piece of gridded card. All wings were intact and did not contain any holes or scarring.

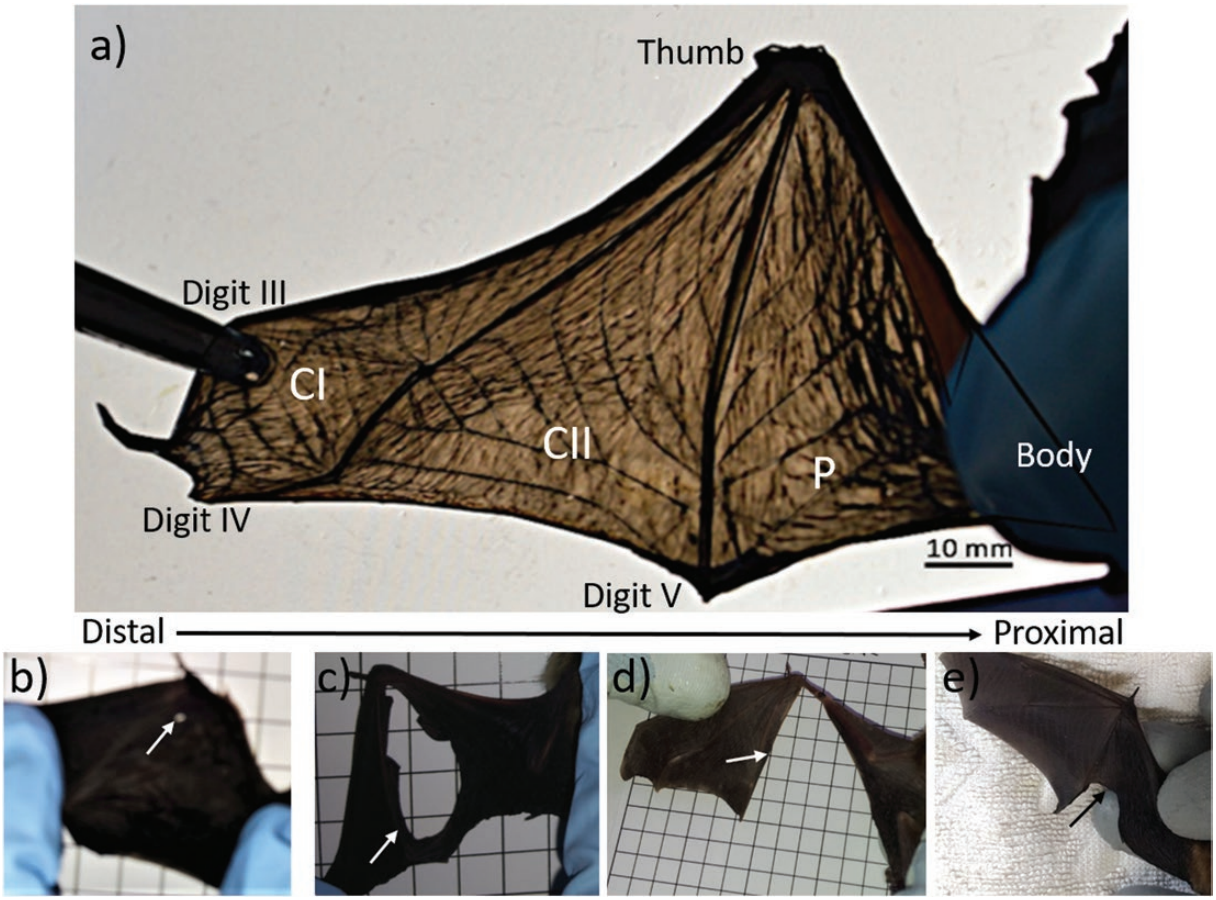

Fig. 1.—Example images of bat wing and tears of common pipistrelles (*Pipistrellus pipistrellus*). a) The wing was stretched over a lightbox to image the blood vessels. The sections of the wing are indicated (CI: the first chiropatagium section; CII: the second chiropatagium section; and P: the plagiopatagium). Examples of the different types of tears are shown, including hole (b), contained tear (c), total tear (d), and trailing edge tear (e).

Inkscape software (https://inkscape.org/en/) was used to trace the blood vessels in all photographs. Some vessels were approximately twice as thick as other vessels, and these were traced with thicker lines. Once the vessels had been drawn in all the photographs, they were combined into one figure to give a summary of all possible blood vessels. This figure was validated against descriptions in the literature (Pavlinić et al. 2008). The number of vessels were counted in each section of the wing (CI, CII, P), and any bifurcations were counted as another vessel. The area of each section of the wing was also measured using Inkscape, to give an approximation of blood vessel density (count/wing area).

Wing histology.—We used Masson's Trichrome staining to identify wing fiber orientation. Two wings from euthanized *P. pipistrellus* were stored in 4% PFA, at 4°C. A fragment from each section of the wing (approximately 10 mm^2) was dissected and sliced tangential to the wing at 30 µm thickness using a freezing cryostat (CM3050, Leica, Wetzlar, Germany) at −20°C. This thickness was selected to reduce the curling and wrinkling of slices that occurred in thinner sections. The slices were transferred to a solution of 10% phosphate-buffered saline (PBS) overnight, mounted on microscope slides (Menzel-Glaser, Thermo Scientific, Braunschweig, Germany), and left to dry for an additional 24 h. The slices were then stained using Masson's Trichrome (Trichrome Stain Kit, Sigma-Aldrich, St. Louis, Missouri). Slides were put in a fixative solution (4% paraformaldehyde in 0.1 M PBS) for 1 h, and introduced to Bouin's Solution for 3 h. They were then cleared with xylene, rehydrated with ethyl alcohol (100, 90, 80, and 70%), and moved through a sequence of solutions for the Masson's Trichrome staining (Biebrich Scarlet Acid, Phosphotungstic and Phosphomolybdic Acids, Aniline Blue, and Acidified Water), with multiple washes of distilled water between each stage. The slices were then dehydrated with ethyl alcohol (70, 90, and 100%) and xylene, towel dried, and cover-slipped using Distyrene Plasticizer Xylene (DPX; Sigma-Aldrich).

To measure relative amounts of collagen and elastin within the sections of the wing, VVG staining was used. Two wings from two euthanized *P. pipistrellus* were stored in 4% PFA, at 4°C. A sample (approximately 10 mm^2) was removed from each section of the wing and placed in 4% PFA overnight at 4°C. Each sample was embedded in 2% agar in PBS and transferred in a histology cassette for tissue processing (Shandon Citadel 2000, Thermo Scientific). Subsequently, the samples were placed in 70% Industrial Methylated Spirits (IMS) for 3 h, 80% IMS for 60 min, 90%

IMS for 60 min, 100% IMS for 2 h twice, 100% IMS for 60 min, then xylene for 90 min twice, xylene for 2 h, and finally in paraffin wax twice for 3 h. Afterwards, the samples were embedded in paraffin wax for slicing. Each sample was sliced across the wing axis (perpendicular to tangential) at 5 µm thickness on an automatic, rotary microtome with water bath (microtome HM355S, Thermo Scientific), collected on glass slides (Superfrost Plus, Thermo Scientific), and incubated in an oven at 37°C overnight before staining. The slides were then cleared with xylene and rehydrated with ethyl alcohol (100%, 90%, 80%, 70%, and distilled water) prior to staining. To stain the elastin, the slides were placed for 10 min in working elastic stain solution, that consisted of 20 ml of hematoxylin solution (HT 251, Sigma-Aldrich), 3 ml ferric chloride solution (HT252, Sigma-Aldrich), 8 ml of Weigert's iodine solution (HT253, Sigma-Aldrich), and 5 ml deionized water. The slides were then rinsed in deionized water and differentiated in ferric chloride solution, comprising of 3 ml ferric chloride solution (HT252, Sigma-Aldrich) and 37 ml of deionized water. Next, the slides were rinsed in tap water, and placed in 95% ethyl alcohol to remove the iodine and then in deionized water. Subsequently, slides were stained for collagen in Van Gieson's solution (Sigma-Aldrich) for 1–3 min, then rinsed in 95% alcohol. Finally, they were dehydrated (100% ethyl alcohol), placed in xylene, and cover-slipped with DPX.

All slices were visualized using a Zeiss Stereo Lumar V12 light microscope (Zeiss, Oberkochen, Germany). Figures were captured using Zeiss Axiovision, version 4.8. Occasional adjustments to exposure and white balance were made. The fiber orientation was described qualitatively for each section stained with Masson's Trichrome. The relative amounts of collagen and elastin were approximated quantitatively using image processing in Matlab from each section stained with VVG. VVG is a standard histological stain used to identify collagen and elastin fibers (Fullmer and Lillie 1956; Kazlouskaya et al. 2013; Cheney et al. 2017), and has been used to quantify amounts of collagen and elastin in stained tissues (Daamen et al. 2003; Raub et al. 2010; Eberson et al. 2015; Wheeler et al. 2015; Lee et al. 2016). Images were selected for image processing when the section was clear and not folded so that all fibers could be seen in the image. Ten to 12 slices were taken

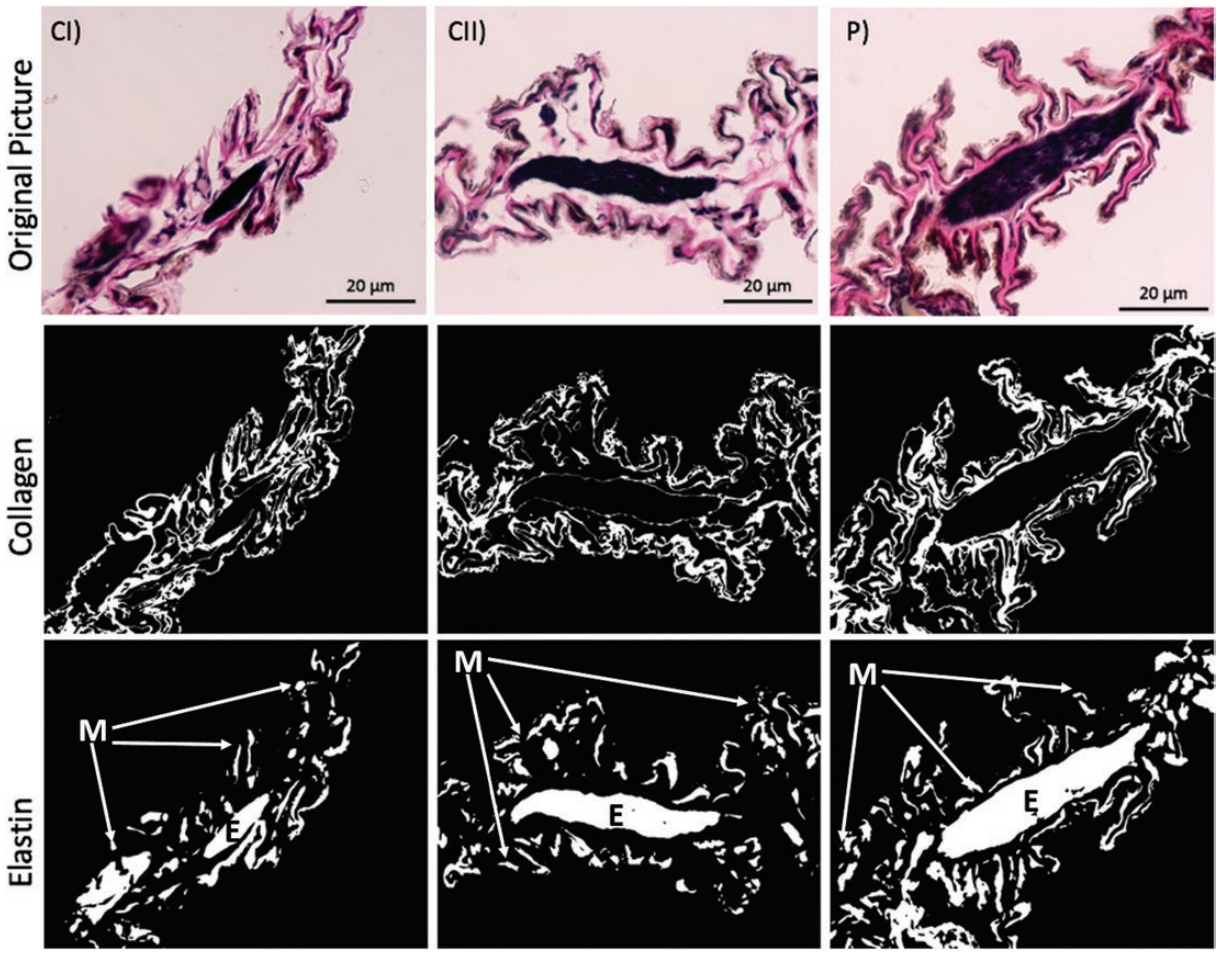

Fig. 2.—Example images demonstrating the processing of elastin and collagen fibers. The top panel shows the original images collected from the microscope following Van Gieson staining. These were processed to find the red-pink collagen colors (middle panels) and the dark elastin colors (bottom panels) for the first chiropatagium section (CI), the second chiropatagium section (CII), and the plagiopatagium section (P). All red-pink pixels were counted for the collagen fibers. For the elastin (E), only the internal elastin fibers were included in the pixel counts; the edges also appeared black in the slices but mainly contained melanin (M), therefore these were cropped from the elastin pixel counts.

for each wing section and then two to three images captured from each slice, giving a total of 35 images for each section.

Original 8-bit color images of the slides reveal collagen as a red-pink color and elastin as a dark, near black color (Fig. 2, top panel; see online version for color). Filters were applied to create two black and white images from each original image, one that showed only collagen and a second showing only elastin (Fig. 2, middle and bottom panels, respectively). A range of filter strengths were tested on the sample images and inspected for accuracy by three independent observers. The position and presence of collagen fibers was also validated by comparing the VVG slices to a subset of slices that were stained with Sirius Red. The settings that provided the most accurate separation of collagen and elastin fibers were then applied to the full image set. Elastin images were created by filtering out pixels with a moderate or high 8-bit color intensity in any RGB channel. Some black color could be seen at the edges of the slices, consisting of melanin in the bat wing skin. Although some elastin was also likely to occur in this area, the edges of the sample were cropped to focus on measuring the internal elastin fibers only (Fig. 2, bottom panels). Collagen images were created by filtering out any pixel with a high green or blue intensity or a low red channel intensity. The red channel threshold was determined automatically (graythresh in Matlab using Otsu's method) on an image-by-image basis taking into account the overall color spectrum of the image. Relative percentages of collagen and elastin were calculated by counting the number of white pixels in each of the generated images.

Material testing.—Ten left wings were used to test the material properties of each wing section; these were all from euthanized bats. Each wing was kept in a freezer at −18°C, and then defrosted in 10% PBS for 10 min. Freezing may have affected the mechanical properties of the samples, and previous studies have shown mixed results (Wang et al. 2007; Kaye 2012) with freezing not having an effect in some cases (Foutz et al. 1992; Van Ee et al. 2000; Santago et al. 2009). As all samples were frozen, we were able to compare between and within samples and observe relative differences, but the absolute values may vary from other studies. After defrosting, long strips were cut out from each wing section, from the digit joint to the trailing edge. The length and width of each strip sample were measured with a ruler (Table 1). The wing thickness was calculated as the mean of three measurements by placing the sample on glass beads and using a microscope (Lumar.V12, Zeiss) with a calibrated camera (AxioCam MRc, Zeiss). Samples were kept hydrated in 10% PBS and tested before drying. Each sample was gripped in a tensometer (Hounsfield H10KS, Tinius Olsen, Horsham, Pennsylvania) using pneumatic grips ensuring consistent grip pressure across all tests. A gauge length of 5 mm was used for all samples, with approximately 11 mm in each grip (refer to average length in Table 1). Each sample was stretched at 10 mm/min until failure, along its longest axis (from the digit joint to the trailing edge). Due to the small size and the delicate nature of the wing of *P. pipistrellus*, the aspect ratios of the tested samples were fairly small and it was not possible to cut a dog-bone shape. Therefore, there were some transverse stresses at the clamps, resulting in wing breakage at the clamp in 30% of the samples, rather than in the middle of the sample. Samples that failed at the grips were removed from further analyses to reduce the effect of incidental bias of transverse stresses on failure stress results. The maximum force at failure (N) and maximum extension (mm) was

Table 1.—Comparing anatomical and material properties of the three wing sections (CI, CII, and P) of common pipistrelles (*Pipistrellus pipistrellus*). Values are mean ± *SD*, *n* refers to the number of bats, and n.a refers to when it was not appropriate to run statistical tests. *P* was considered significant at the < 0.01 level, with a Bonferroni correction (indicated in bold).

	Wing section			
	CI	CII	P	Statistics
Blood vessels				
Number	14.00 ± 1.70	12.60 ± 1.51	9.00 ± 1.56	$\chi^2 = 18.686$, $P <$ **0.001** (CI, CII > P), $n = 10$
Density (no./cm^2)	2.16 ± 0.99	0.98 ± 0.54	0.63 ± 0.48	$\chi^2 = 13.628$, $P =$ **0.001** (CI > CII, P), $n = 10$
Fibers				
% Collagen	79.92 ± 13.73	43.09 ± 21.78	52.47 ± 26.95	$\chi^2 = 35.922$, $P <$ **0.001** (CI > CII, P), $n = 2$
% Elastin	20.08 ± 13.73	56.91 ± 21.78	47.53 ± 26.95	$\chi^2 = 35.922$, $P <$ **0.001** (CI < CII, P), $n = 2$
Material properties				
Section length (mm)	33.60 ± 7.97	26.66 ± 7.45	26.02 ± 5.79	n.a
Section width (mm)	2.83 ± 1.18	4.59 ± 0.96	5.60 ± 1.38	n.a
Section depth (mm)	0.22 ± 0.04	0.24 ± 0.02	0.33 ± 0.04	$\chi^2 = 13.569$, $P =$ **0.001** (CI, CII < P), $n = 7$
Failure stress (N/mm^2)	2.32 ± 0.81	2.48 ± 0.94	1.58 ± 0.61	$\chi^2 = 4.364$, $P = 0.113$ $n = 7$
Failure strain (mm/mm)	0.37 ± 0.110	0.61 ± 0.182	0.63 ± 0.20	$\chi^2 = 9.062$, $P =$ **0.011** (CI < CII, P), $n = 7$
Young's modulus (N/mm^2)	8.07 ± 2.19	6.22 ± 3.12	4.45 ± 1.97	$\chi^2 = 6.033$, $P = 0.049$ (CI > P), $n = 7$
Component stiffness (N/mm)	1.37 ± 0.29	1.10 ± 0.61	0.93 ± 0.55	$\chi^2 = 2.879$, $P = 0.237$ $n = 7$

recorded. From these values, failure stress (force at failure divided by the cross-sectional area), failure strain (maximum extension divided by the original sample length of 5 mm), and Young's modulus (change in stress divided by the change in strain) were all calculated for each sample from each wing section. As strips from the P section tended to be wider than those from the other sections (Table 1), component stiffness (force at failure divided by sample width, divided by failure strain) was also calculated to control for sample width but not thickness. Results were quasi-linear and did not exhibit the 2-part loading curve, with "toe" and "upturn" regions, demonstrated by Skulborstad et al. (2015); therefore, a single gradient was calculated from the major linear region of each stress–strain curve.

Wing tear photographs.—Data on bat wing tears were collected over 20 months between March 2016 and October 2017 from live, rehabilitating animals. Photographs of torn wings were collected from bat rehabilitators soon after the bat was admitted to care. Bat rehabilitators were recruited by advertising the project at the Mammal Society Easter Meetings, the National Bat Conference, the National Bat Care Conference, and in Bat Care News, as well as from Facebook groups across the United Kingdom (UK Bat Workers, Cambridgeshire Bat Group, Kent Bat Group, and South Lancashire Bat Group). Soon after admittance, bat rehabilitators were also asked to describe how the bat was found and the possible cause of the tear. Bat rehabilitators emailed comments on the possible cause, describing any evidence for their decision. Fifty-five pictures of *P. pipistrellus* and 21 pictures of other United Kingdom bat species were collected, including two brown long-eared bats (*Plecotus auritus*), three Natterer's bats (*Myotis nattereri*), one serotine bat (*Eptesicus serotinus*), 12 soprano pipistrelles (*Pipistrellus pygmaeus*), and three whiskered bats (*Myotis mystacinus*). The wing tears were photographed while the bat was awake (not during torpor nor under anesthetic), and its wing was extended and held against a gridded card for scale. From each image, every tear was traced as it appeared in the photograph using Inkscape onto a wing diagram, and coded by color for the frequency of its occurrence in that location. The total number of all tears in each section of the wing was also determined. In addition, the tears were categorized into four major types, based on criteria of classification that were developed during this study: holes, contained tears, total tears, and trailing edge tears. A hole is a small puncture, it can be round or oval, and is usually not more than 2% of a wing segment (Fig. 1b). A contained tear is larger than a hole. It is a tear, rather than a puncture, that is still entirely contained within the wing (Fig. 1c). It can also be round or oval, with 5–50% of the membrane missing from a wing segment. A total tear is a tear that runs from the internal membrane to the trailing edge of the wing (Fig. 1d), thus not being contained within the wing. It often has a vertical appearance (like a triangle), and the bones are often affected or missing; more than 50% of the membrane tends to be missing from the wing segment. A trailing edge tear is horizontal in appearance and occurs only at the trailing edge of the wing (Fig. 1e). Some variation existed in how much the wing was stretched in each photograph (Figs. 1b–e). For example, sometimes other injuries prevented the rehabilitator from fully extending the wing. This may have influenced some classifications of holes and contained tears. However, holes did not have any further ripping, and were puncture wounds (Fig. 1b), whereas contained tears tended to be much larger and ragged around the edges, from ripping (Fig. 1c).

Bat rehabilitators were approached 9–12 months after submitting their photographs and asked what the outcome of the rehabilitation was. No further photographs were collected at this follow-up. Recommendations for bat rehabilitators for release, rehabilitation, and euthanasia practices are provided by the BCT and the Department for Environment, Food and Rural Affairs (DEFRA—Mitchell-Jones and McLeish 2004; Miller 2016), but are not quantitative, and rely on the experience and opinions of the individual rehabilitators. Bat rehabilitators emailed comments detailing how long the bat was in care before release, whether they were still in care, or were euthanized. These data were collected and, upon review, fell naturally in to four categories: released after 2 weeks, released within 2–3 months, still in care after 6 months, and euthanized. These follow-up data were collected from 13 common pipistrelles (*P. pipistrellus*), and 15 other species of United Kingdom bats, including 12 soprano pipistrelles (*P. pygmaeus*), one Natterer's bat (*M. nattereri*), one brown long-eared bat (*P. auritus*), and one serotine bat (*E. serotinus*).

Statistical considerations.—The three sections of the wing were compared for the following variables: number of blood vessels, density of blood vessels (number/cm^2), section thickness (mm), stress (N/mm^2), strain (mm/mm), Young's modulus (N/mm^2), component stiffness (N/mm), % collagen, and % elastin. They were compared using a Kruskal–Wallis test, with wing section as the dependent variable. Pairwise comparisons were undertaken using Mann–Whitney tests in SPSS (IBM SPSS Statistics, version 24, Armonk, New York), and are all summarized in Table 1, with a Bonferroni correction applied at the $P < 0.01$ level of significance. Total tear numbers and tear types were compared for *P. pipistrellus* between each of the three wing sections using a chi-square test. In other United Kingdom bat species, only the total tear numbers were tested with a chi-square test for each of the wing sections, and there were many zero scores in the tear type data. Sample sizes for the follow-up healing data were too small for statistical analysis, but are presented graphically for comparison.

Results

Blood vessels.—Section P had significantly fewer blood vessels than sections CI and CII of the bat wing (Table 1, $P < 0.01$); from our observations, it also appeared to have the thickest blood vessels, as indicated by the thicker lines in Fig. 3 (see also Fig. 1a). However, section P was also the largest section. When the number of blood vessels was normalized to the area of each wing section, there was no significant difference in blood vessel density between sections P and CII (Table 1), but section CI had the densest arrangement of blood vessels (Table 1, $P < 0.01$).

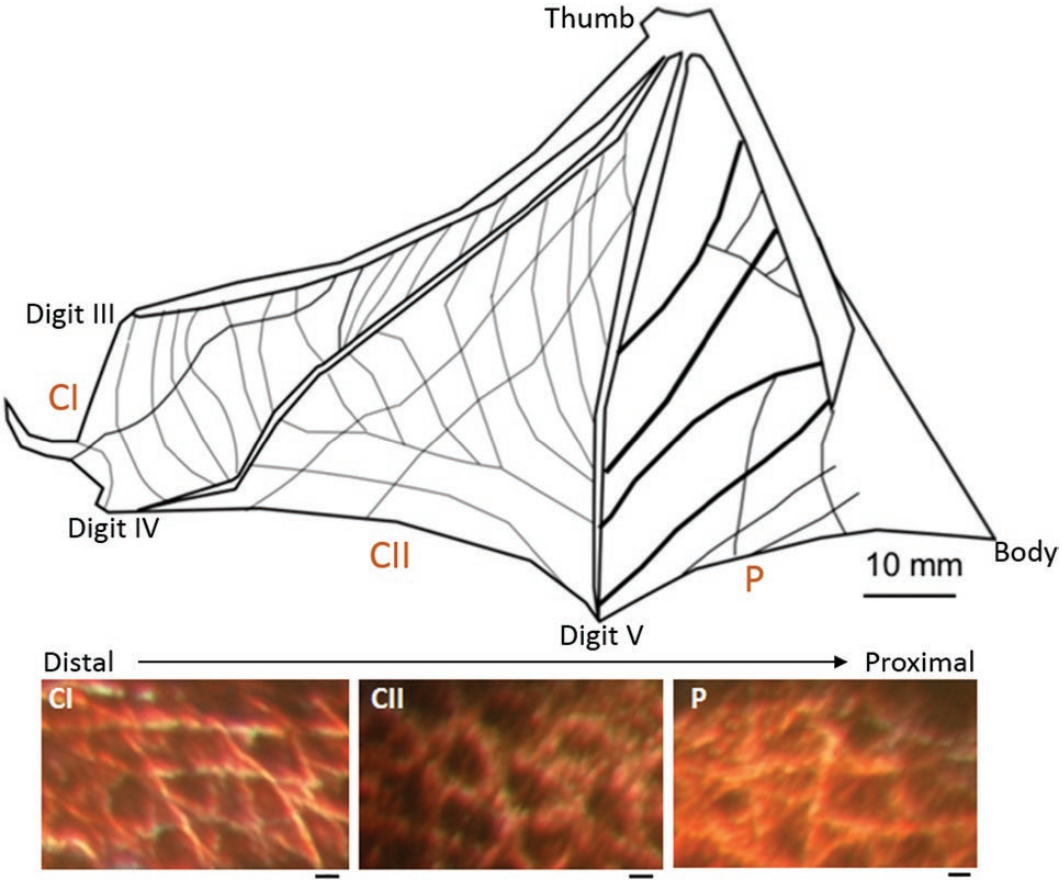

Fig. 3.—Bat wing anatomy. Top: Blood vessel tracing for common pipistrelle (*P. pipistrellus*) wings; thicker lines correspond to vessels that are twice as thick as others. Digits III, IV, and V are also indicated on the figure; digit II is not visible as it is folded against digit III, and digit I is the thumb. Bottom: Fiber orientations (elastin and collagen) for the first chiropatagium section (CI), the second chiropatagium section (CII), and the plagiopatagium section (P). Scale bars are 0.1 mm.

Wing fibers.—The orientation of fibers within the wing tended to be multidirectional and distributed in a net-like fashion throughout the membrane, with a similar appearance in each wing section (Fig. 3). The appearance of the fibers at many orientations indicates the material is, at least visually, isotropic. The amount of collagen (%) was significantly higher in section CI and the amount of elastin (%) was significantly lower in section CI, compared to sections CII and P (Table 1, $P < 0.01$).

Material testing.—Section P was the thickest section (Table 1, $P < 0.05$). No significant differences were observed between the wing sections for any of the material-testing measurements (Table 1), although CI tended to have the smallest deformation (failure strain) and highest Young's modulus (compared to section P), and section P tended to have the lowest failure stress and component stiffness (Table 1).

Characterizing wing tears.—There were more wing tears in the P section than in CI and CII in *P. pipistrellus* ($\chi^2 = 18.951$, $P < 0.01$, Figs. 4a, c, and e). The types of tears did not differ significantly between wing sections in *P. pipistrellus* ($\chi^2 = 3.647$, $P = 0.161$, Figs. 4c and e). Holes were the most common tear type in all wing sections and appeared distributed fairly evenly in each wing section. The contained and total tears tended to be oriented rostro-caudally, from an internal part of the wing membrane toward the trailing edge (Fig. 4c), and occurred more prevalently in the proximal wing sections (Figs. 4c and e). Bat rehabilitators gave possible causes for 11 of 55 individuals. One individual was bought in to the house by a cat, four were seen being attacked by a cat (Fig. 5a), and five were suspected by the rehabilitators to be cat attacks. One individual was found on the ground and was likely to have sustained tears from brambles on the ground surface (Fig. 5b), and had tears throughout each section of the wing.

Other bat species (all species pooled) also had significantly more wing tears in the P section than in CI and CII ($\chi^2 = 8.773$, $P = 0.012$; Figs. 4b, d, and f). Holes and contained tears were common tear types, and section P was the only section to reveal all the possible tear types. Tear types were commonly oriented in the rostro-caudal direction, from the membrane to the trailing edge, with only section P revealing one trailing edge tear that was oriented distal-proximally. Bat rehabilitators gave possible causes for seven of 21 individuals. One was seen being attacked by a cat, and two were suspected by the rehabilitators to be cat attacks (Fig. 5c). One bat was caught in flypaper and three were seen in a cat's mouth (Fig. 5d).

Sample numbers reporting rehabilitation outcomes were low and not analyzed statistically. Larger tears in CI did not affect the length of time that *P. pipistrellus* spent in care (Fig. 6).

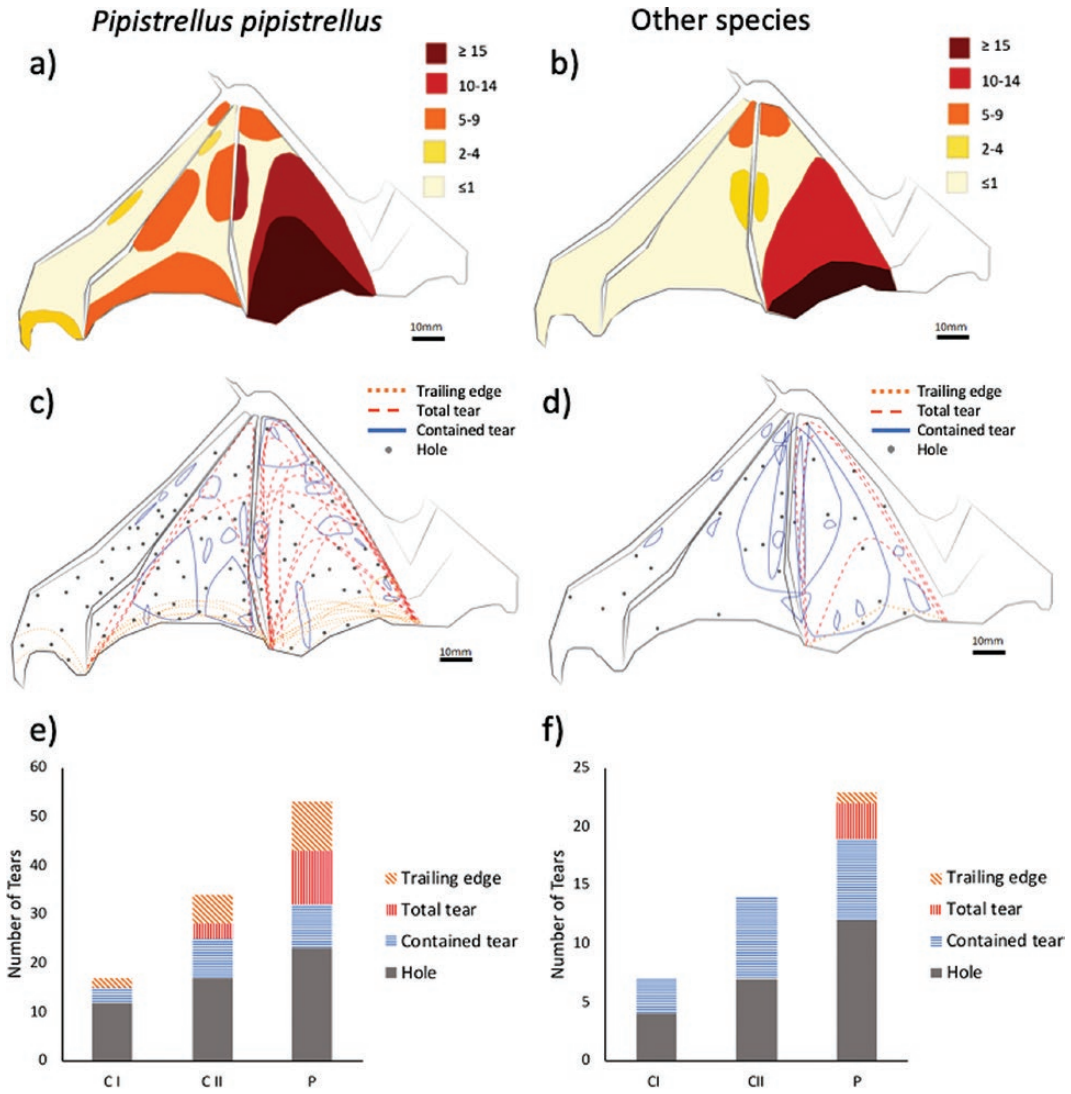

Fig. 4.—Characterization of bat wing tears. Left hand panels are data from *P. pipistrellus*, and the right hand panels are from other United Kingdom bat species. Panels (a) and (b) show the numbers of tears in each section of the wing. Panels (c) and (d) show all the wing tear positions of all tear types on each section of the wing, with dashed lines indicating total tears, dotted lines indicating trailing edge tears, solid lines indicating contained tears, and gray dots as holes. Panels (e) and (f) show the total numbers of different tear types in each wing section for the first chiropatagium section (CI), the second chiropatagium section (CII), and the plagiopatagium section (P)).

However, larger tears in P could be seen in the bat that was still in care after 6 months (Fig. 6a). In addition, large tears in both CII and P were found in the euthanized *P. pipistrellus* (Fig. 6a). In other species, large tears in section P were found in the two bats that were still in care after 6 months (Fig. 6b), but tear size did not vary much between the other wing sections in euthanized bats, or those released after 2 weeks and 2–3 months (Fig. 6b).

Discussion

The plagiopatagium section (P) sustained the most injuries. We suggest that section P, being close to the body, is likely to be torn by predators targeting the body. Furthermore, cat attacks might be causing many of the rostro-caudal tears in the P section. We consider tearing capacity and suggest that, according to its anatomy, section P should not be more prone to tearing than any other section. Therefore, the position of section P, rather than its anatomy, is an important factor in determining the number, location, and orientation of wing tears.

Position of tearing.—Across all species, section P contained the highest number and most varied types of tears (Fig. 4). Most figures in Davis (1968) also revealed that torn wings or large holes in Pallid bats (*A. pallidus*) were common in section P, with CI and CII having more trailing edge tears. There are several reasons for the greater number of tears in section P. It is the largest section of the wing and perhaps more likely to tear. It also contains the fewest bones (Fig. 1a), which may act to stop tearing. Section P is extended first before flight and might get caught or snagged during flight preparation (see figure 1 in Gardiner et al. 2011). Our consideration of anatomical properties (fiber type and material testing data) within section

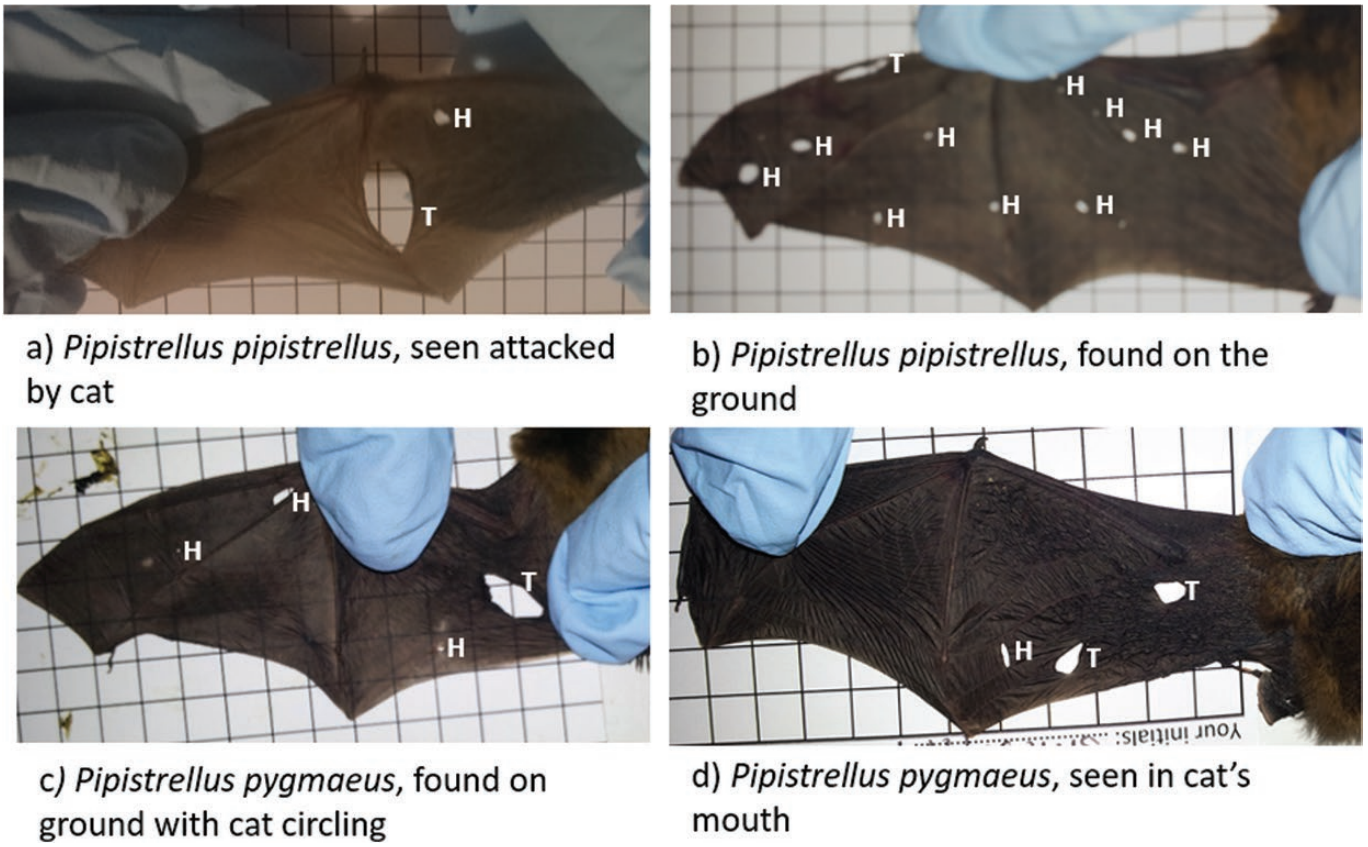

Fig. 5.—Example wing tears, with associated causes. Confirmed cat attacks cause damage to the proximal wing sections (section P) in *P. pipistrellus* (a) and *P. pygmaeus* (c and d). Grounded bats have damage to other areas of the wing in *P. pipistrellus* (b) and *P. pygmaeus* (c). Tears in these photographs were categorized as holes (H) and contained tears (T). Some pale marks can also be seen in image (b) and (c), which are healed tears.

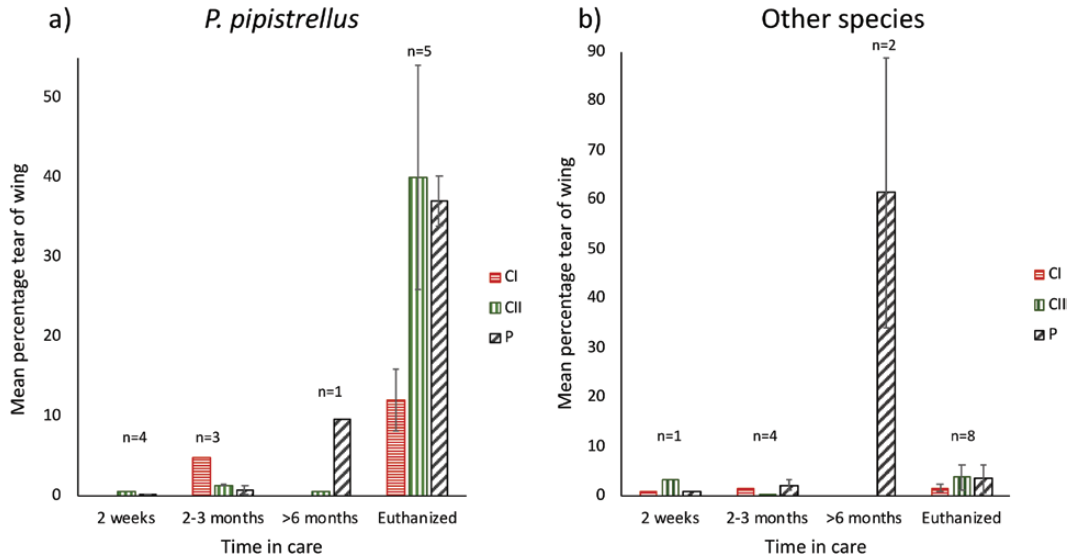

Fig. 6.—Time in rehabilitation from follow-up data. Panels (a) and (b) show the length of time that bats were in care, when they received a tear in a wing section. Percentage of the wing section torn or missing is on the y-axis, and mean values are presented with *SE* bars. *n* represents the number of bats in that classification.

P suggests it should not be more prone to tearing than sections CI and CII.

Within a bat wing, elastin fibers run perpendicular to the wing bones, and collagen fibers create a network parallel and perpendicular to the elastin, which has been described in a number of studies (Holbrook and Odland 1978; Madej et al. 2012; Cheney et al. 2015, 2017). This net-like fiber array provides tensile strength and limits extension of the wing membranes, which is important for flight (Holbrook and Odland 1978). We observed a fibrous net that has a similar appearance in each section of the

wing (Fig. 3). This net might act to limit tears from extending, and maintain holes as small holes rather than tearing further. Its equal distribution reinforces the entire wing surface (Holbrook and Odland 1978). That this net does not appear to differ between the three wing sections indicates that they should each be similarly resistant to tearing.

Quasi-static material testing and analysis of collagen-elastin percentages were carried out to compare the three wing sections further. Section CI had significantly higher relative collagen percentages than the other wing sections (% collagen, Table 1) and tended to exhibit the least extension (failure strain, Table 1, although not significant $P > 0.01$). Sections CII and P exhibited more equal collagen-elastin ratios and consequently failed at lower stress values and underwent greater extension. However, when accounting for the increased thickness of the CII and P section, no significant difference was found in the component stiffness of any of the three sections. Component stiffness normalizes for the dissected width of tested samples but allows for the natural variation in thickness of the wing sections. The similarity of values across CI, CII, and P suggests that no one section is inherently "easier" to induce failure in than any other. The P section, while weak as a pure material, requires a similar force to break when viewed as a component. The higher relative percentages of elastin in the CII and P sections may be an adaptation to improve wing folding. As the largest and most proximal sections, they are required to unfurl (stretch out) the most during flight, and higher levels of elastin should benefit this function (Cheney et al. 2015).

A study on seven species of non-*Pipistrellus* bats by Swartz et al. (1996) found that the plagiopatagium was the weakest wing section overall, was thicker, had the lowest Young's modulus, and stretched the most before breaking. This fits the general trend in our data. However, we did not observe significant differences in these parameters. Patterns in material properties varied between the different wing sections across bat genera (see figure 9 in Swartz et al. 1996), which might explain why our results differed, as they did not measure *Pipistrellus* sp. We also observed variation within individuals (note high *SD* values in material property data in Table 1).

Orientation of tears.—Despite presence of the fibrous net in all wing sections, many tears occurred in a rostro-caudal orientation, especially in section P. This coincides with the direction of travel, and might be indicative of the bat wing being snagged while moving forward. Proximal-distal tears tended to occur only around the trailing edges of the wings (Figs. 4c and d), despite being reinforced here by bundles of skeletal muscle fibers (Holbrook and Odland 1978).

If the wing is isotropic when it is stretched out, it should be equally susceptible to tearing in every orientation. Bat wings were thought to be highly anisotropic (Swartz et al. 1996). However, the elastin accounts for much of this difference and once the elastin has "unwrinkled," the wing is isotropic (Cheney et al. 2015). Therefore, our force results are likely representative of the wing as a whole, regardless of orientation of the sample, although displacement will be significantly higher in samples perpendicular with ours, as the elastin stretches out (unwrinkles).

Implications for healing.—While anatomy of the wing is not associated with the position and orientation of tears, it may affect healing. Indeed, Faure et al. (2009) suggested that tears healed quicker in the uropatagium than the chiropatagium due to its extensive vasculature. If so, our results suggest that tears to section P may take the longest time to heal. Section CI has the highest density of blood vessels, while section P has the lowest number of blood vessels (Fig. 3; Table 1), which occurs as the vessels naturally bifurcate from proximal to distal.

Extensive vasculature is associated with increased healing capabilities in bat wings and tails (Faure et al. 2009), with both the wound and scarring healing quicker. Blood carries factors to the wound site to clean the wound, prevent infection, and begin the process of reforming the tissue matrix. Therefore, being close to a vessel is likely to be important for quick healing, which has also been suggested by Faure et al. (2009) and Pollock et al. (2016). As CI had the most extensive vasculature, we expect it to heal quicker than section P. While section P had the lowest numbers of blood vessels, it also had the thickest vessels. These supply blood to the thinner, branched, more densely distributed vessels in the other sections of the wing. Following a tear, these thicker vessels might bleed more, and lead to additional complications. The majority of tears occurred on section P of the wing, which is likely to be the slowest to heal.

We did not measure healing rates in this study. However, our follow-up data on rehabilitation outcomes suggest that larger tears in section P were found in *P. pipistrellus* individuals that spent a long time in care (> 6 months) or were euthanized, although the sizes of tears were large in all wing sections in animals that were euthanized (Fig. 6). In other United Kingdom bat species, the individuals that spent a long time in care (> 6 months) also had large tears in the P section. Decisions about release, rehabilitation, and euthanasia are highly subjective and are dependent not only on the extent of injury, but also on the judgment of the bat rehabilitator, season, and weather conditions. Linking our tear characterization method with detailed information about healing rates and post-release survival will help to develop stricter rehabilitation recommendations.

Greville et al. (2018) found that in the Egyptian fruit bat (*Rousettus aegyptiacus*) wounds took about 1.5 days longer to heal to 50% wound closure in section P, compared to the chiropatagium (sections CI and CII), although this was not found in the big brown bat (*E. fuscus*). They suggest that not just blood vessels, but also collagen and elastin fibers are likely to play a role in healing. Indeed, Greville et al. (2018) suggest that over-stretching of the collagen or elastin fibers during healing can cause the tear to enlarge before healing. This phenomenon also was observed in tail and wing membranes by Pollock et al. (2016). We suggest that proximal-distal orientation of elastin fibers may hold the common rostro-caudal tears apart, thus increasing healing times. This will be especially true in the P section, which has a lot of elastin and is the largest wing section with the most movement. It also undergoes the most wrinkling when

folded against the body. Tears in this section may be stretched and extended the most during the healing process.

Implications for survival.—Section P supports the bat's body during flight and provides lift (Vaughan 1970; Swartz et al. 1996; Neuweiler 2000), while the CI and CII sections provide thrust (Swartz et al. 1996; Neuweiler 2000). Therefore, damage to different sections of the wing can affect flight differently. Tears in the CI or CII sections are likely to affect maneuverability and speed, while tears in the P section may inhibit bats' ability to generate lift. However, bats do fly with large tears in their wings (Davis 1968). Voigt (2013) studied two species of *Myotis* with unilateral trailing edge tears of approximately 20% in section P and found that injured bats made fewer flight maneuvers and had lower metabolic rates than healthy individuals. Thus, foraging success and survival are likely affected by limited flight maneuverability. Large wing tears can prevent flight altogether. Grounded bats are likely to sustain wing tears from thorns and other ground matter (Davis 1968). This may explain the tears in all wing sections in severely injured bats that were euthanized (Fig. 6). Indeed, wound healing is just the first step in a long rehabilitation process. While some studies have monitored *Pipistrellus* species post-release (Kelly et al. 2008, 2012; Serangeli et al. 2012), these have been relatively short term and not focused on wing tears. Further investigations of the effect of wing tears on flight capabilities, foraging, and survival, especially post-release, will help us to understand both the long-term effects of wing injuries and benefits of rehabilitation.

Possible causes of wing tears.—Each section of the wing is equally disposed to tearing in any orientation, despite the prevalence of many rostro-caudal tears in the P section. We suggest that it is the position of section P, rather than its anatomy, that makes it more likely to tear. Wing tears and holes can occur as a result of collisions with objects or plants with thorns (Davis 1968), fungal infections (Reichard and Kunz 2009; Cryan et al. 2010; Fuller et al. 2011), or predator attacks, including those by cats (Ancillotto et al. 2013; Loss et al. 2013; Russo and Ancillotto 2015) and birds of prey (Speakman 1991). Puncture wounds may also be caused by interspecific (Brokaw et al. 2016) or intra-specific aggression (such as in roost sites), which is likely to occur across the whole wing surface, including P, CI, and CII. Collisions are more likely to produce holes or tears on the distal wing sections (i.e., section CI), and may be oriented rostro-caudally, in the direction of flight. Tears in section P can be holes and horizontal trailing edge tears, but many are rostro-caudal, starting from the middle of the wing and extending to the trailing edge. We suggest that holes or tears in wing sections proximal to the body may be caused by predators, including cat attacks and perhaps failed talon strikes by birds like barn owls (*Tyto alba*—Speakman 1991). Indeed, the position and orientation of many tears in the plagiopatagium were consistent with the notion that predators direct their attacks toward the body of the bat, as this is the wing section that is closest to the body. Ancillotto et al. (2013) found that predation by cats accounted for 28.7% of adult bats admitted to rehabilitation centers. Identifying the causes of wing tears will help us to understand both the scale of the problem and enable us to design prevention strategies and management procedures.

Acknowledgments

Many thanks to all the bat rehabilitators that supplied photographs for the study. Special thanks to H. Ryan and S. Humphreys, who supplied the majority of our samples, and M. Brown, who advertised our study in Bat Care News. We are grateful to J. Horton for helping to develop the tear classification system as part of her MSc project. Thanks to T. Allen and M. Green for their support with the material testing, and R. Peters for assistance with the histology work. We are also extremely grateful to the AniMAS (Animal Motion and Sensing) Lab reading group for their comments on the manuscript. We are grateful to the Saudi Arabia Cultural Bureau (#16306087) for funding a PhD studentship for ROSK which this work was carried out as part of.

Literature Cited

Aegerter, J., D. Fouracre, and G. C. Smith. 2017. A first estimate of the structure and density of the populations of pet cats and dogs across Great Britain. PLoS ONE 12:1–21.

Ancillotto, L., M. T. Serangeli, and D. Russo. 2013. Curiosity killed the bat: domestic cats as bat predators. Mammalian Biology 78:369–373.

Brokaw, A. F., J. Clerc, and T. J. Weller. 2016. Another account of interspecific aggression involving a hoary bat (*Lasiurus cinereus*). Northwestern Naturalist 97:130–134.

Ceballos-Vasquez, A., J. R. Caldwell, and P. A. Faure. 2015. Seasonal and reproductive effects on wound healing in the flight membranes of captive big brown bats. Biology Open 4:95–103.

Cheney, J. A., J. J. Allen, and S. M. Swartz. 2017. Diversity in the organization of elastin bundles and intramembranous muscles in bat wings. Journal of Anatomy 230:510–523.

Cheney, J. A., N. Konow, A. Bearnot, and S. M. Swartz. 2015. A wrinkle in flight: the role of elastin fibres in the mechanical behaviour of bat wing membranes. Journal of the Royal Society Interface 12:20141286.

Church, J. C., and D. J. Warren. 1968. Wound healing in the web membrane of the fruit bat. The British Journal of Surgery 55:26–31.

Cryan, P. M., C. U. Meteyer, J. G. Boyles, and D. S. Blehert. 2010. Wing pathology of white-nose syndrome in bats suggests life-threatening disruption of physiology. BMC Biology 8:135.

Daamen, W. F., et al. 2003. Preparation and evaluation of molecularly-defined collagen-elastin-glycosaminoglycan scaffolds for tissue engineering. Biomaterials 24:4001–4009.

Davis, R. 1968. Wing defects in a population of pallid bats. The American Midland Naturalist 79:388–395.

Davis, R., and S. E. Doster. 1972. Wing repair in pallid bats. Journal of Mammalogy 53:377–378.

Eberson, L. S., P. A. Sanchez, B. A. Majeed, S. Tawinwung, T. W. Secomb, and D. F. Larson. 2015. Effect of lysyl oxidase inhibition on angiotensin II-induced arterial hypertension, remodeling, and stiffness. PLoS ONE 10:e0124013.

Faure, P. A., D. E. Re, and E. L. Clare. 2009. Wound healing in the flight membranes of big brown bats. Journal of Mammalogy 90:1148–1156.

Foutz, T. L., E. A. Stone, and C. F. Abrams, Jr. 1992. Effects of freezing on mechanical properties of rat skin. American Journal of Veterinary Research 53:788–792.

Fuller, N. W., J. D. Reichard, M. L. Nabhan, S. R. Fellows, L. C. Pepin, and T. H. Kunz. 2011. Free-ranging little brown myotis

(*Myotis lucifugus*) heal from wing damage associated with white-nose syndrome. EcoHealth 8:154–162.

Fullmer, H. M., and R. D. Lillie. 1956. The staining of collagen with elastin tissue stains. Journal of Histochemistry and Cytochemistry 4:11–14.

Gardiner, J. D., G. Dimitriadis, J. R. Codd, and R. L. Nudds. 2011. A potential role for bat tail membranes in flight control. PLoS ONE 6:e18214.

Greville, L. J., A. Ceballos-Vasquez, R. Valdizón-Rodríguez, J. R. Caldwell, and P. A. Faure. 2018. Wound healing in wing membranes of the Egyptian fruit bat (*Rousettus aegyptiacus*) and big brown bat (*Eptesicus fuscus*). Journal of Mammalogy 99:974–982.

Hale, J. D., A. J. Fairbrass, T. J. Matthews, G. Davies, and J. P. Sadler. 2015. The ecological impact of city lighting scenarios: exploring gap crossing thresholds for urban bats. Global Change Biology 21:2467–2478.

Hale, J. D., A. J. Fairbrass, T. J. Matthews, and J. P. Sadler. 2012. Habitat composition and connectivity predicts bat presence and activity at foraging sites in a large UK conurbation. PLoS ONE 7:e33300.

Holbrook, K. A., and G. F. Odland. 1978. A collagen and elastic network in the wing of the bat. Journal of Anatomy 126(Pt 1):21–36.

Jung, K., and C. G. Threlfall. 2018. Trait-dependent tolerance of bats to urbanization: a global meta-analysis. Proceedings of the Royal Society B: Biological Sciences 285:20181222.

Kaye, B. 2012. The effects of freezing on the mechanical properties of bone. The Open Bone Journal 4:14–19.

Kazlouskaya, V., S. Malhotra, J. Lambe, M. H. Idriss, D. Elston, and C. Andres. 2013. The utility of elastic Verhoeff-Van Gieson staining in dermatopathology. Journal of Cutaneous Pathology 40:211–225.

Kelly, A., S. Goodwin, A. Grogan, and F. Mathews. 2008. Post-release survival of hand-reared pipistrelle bats (*Pipistrellus* spp.). Animal Welfare 17:375–382.

Kelly, A., S. Goodwin, A. Grogan, and F. Mathews. 2012. Further evidence for the post-release survival of hand-reared, orphaned bats based on radio-tracking and ring-return data. Animal Welfare 21:27–31.

Lee, L., et al. 2016. Aortic and cardiac structure and function using high-resolution echocardiography and optical coherence tomography in a mouse model of Marfan syndrome. PLoS ONE 11:1–19.

Lintott, P. R., et al. 2015. Differential responses to woodland character and landscape context by cryptic bats in urban environments. PLoS ONE 10:e0126850.

Loss, S. R., T. Will, and P. P. Marra. 2013. The impact of free-ranging domestic cats on wildlife of the United States. Nature Communications 4:1396.

Madej, J. P., et al. 2012. Skin structure and hair morphology of different body parts in the common pipistrelle (*Pipistrellus pipistrellus*). Acta Zoologica 94:478–489.

Mehr, M., R. Brandl, T. Hothorn, F. Dziock, B. Förster, and J. Müller. 2011. Land use is more important than climate for species richness and composition of bat assemblages on a regional scale. Mammalian Biology 76:451–460.

Mendes, E. S., M. J. R. Pereira, S. F. Marques, and C. Fonseca. 2014. A mosaic of opportunities? Spatio-temporal patterns of bat diversity and activity in a strongly humanized Mediterranean wetland. European Journal of Wildlife Research 60:651–664.

Miller, H. (ed.). 2016. Bat care guidelines. 2nd ed. The Bat Conservation Trust, London, United Kingdom.

Mitchell-Jones, A. J., and A. P. Mcleish. 2004. Bat workers manual. 3rd ed. Joint Nature Conservation Committee, Peterborough.

Molony, S. E., P. J. Baker, L. Garland, I. C. Cuthill, and S. Harris. 2007. Factors that can be used to predict release rates for wildlife casualties. Animal Welfare 16:361–367.

Moorhouse, T. P., M. Gelling, G. W. McLaren, R. Mian, and D. W. Macdonald. 2007. Physiological consequences of captive conditions in water voles (*Arvicola terrestris*). Journal of Zoology 271:19–26.

Neuweiler, G. 2000. The biology of bats. Oxford University Press, New York.

Pavlinić, I. G. O. R., N. I. Tvrtković, and D. R. Holcer. 2008. Morphological identification of the soprano in Croatia. Hystrix 19:47–53.

Pollock, T., C. R. Moreno, L. Sánchez, A. Ceballos-Vasquez, P. A. Faure, and E. C. Mora. 2016. Wound healing in the flight membranes of wild big brown bats. Journal of Wildlife Management 80:19–26.

Powers, L. E., J. E. Hofmann, J. Mengelkoch, and B. M. Francis. 2013. Temporal variation in bat wing damage in the absence of white-nose syndrome. Journal of Wildlife Diseases 49:946–954.

Raub, C. B., S. Mahon, N. Narula, B. J. Tromberg, M. Brenner, and S. C. George. 2010. Linking optics and mechanics in an in vivo model of airway fibrosis and epithelial injury. Journal of Biomedical Optics 15:015004.

Reichard, J. D., and T. H. Kunz. 2009. White-nose syndrome inflicts lasting injuries to the wings of little brown myotis (*Myotis lucifugus*). Acta Chiropterologica 11:457–464.

Russo, D., and L. Ancillotto. 2015. Sensitivity of bats to urbanization: a review. Mammalian Biology 80:205–212.

Santago, A. C., A. R. Kemper, C. McNally, J. L. Sparks, and S. M. Duma. 2009. Freezing affects the mechanical properties of bovine liver. Biomedical Sciences Instrumentation 45:24–29.

Santini, L., M. González-Suárez, D. Russo, A. Gonzalez-Voyer, A. von Hardenberg, and L. Ancillotto. 2019. One strategy does not fit all: determinants of urban adaptation in mammals. Ecology Letters 22:365–376.

Serangeli, M., L. Cistrone, L. Ancillotto, A. Tomassini, and D. Russo. 2012. The post-release fate of hand-reared orphaned bats: survival and habitat selection. Animal Welfare 21:9–18.

Sikes, R. S., and the Animal Care and Use Committee of the American Society of Mammalogists. 2016. 2016 Guidelines of the American Society of Mammalogists for the use of wild mammals in research and education. Journal of Mammalogy 97:663–688.

Skulborstad, A. J., S. M. Swartz, and N. C. Goulbourne. 2015. Biaxial mechanical characterization of bat wing skin. Bioinspiration & Biomimetics 10:036004.

Speakman, J. R. 1991. The impact of predation by birds on bat populations in the British Isles. Mammal Review 21:123–142.

Studier, E. H. 1972. Some physical properties of the wing membranes of bats. Journal of Mammalogy 53:623–625.

Swartz, S. M., M. D. Groves, H. D. Kim, and W. R. Walsh. 1996. Mechanical properties of bat wing membrane skin: aerodynamic and mechanical functions. Journal of Zoology, London 239:357–378.

Van Ee, C. A., A. L. Chasse, and B. S. Myers. 2000. Quantifying skeletal muscle properties in cadaveric test specimens: effects of mechanical loading, postmortem time, and freezer storage. Journal of Biomechanical Engineering 122:9–14.

Vaughan, T. A. 1970. The muscular system. Pp. 139–194 in Biology of bats. 1st ed. (W. A. Wimsatt, eds). Academic Press, New York.

Voigt, C. C. 2013. Bat flight with bad wings: is flight metabolism affected by damaged wings? Journal of Experimental Biology 216:1516–1521.

Wang, D., W. Ma, Y. Niu, X. Chang, and Z. Wen. 2007. Effects of cyclic freezing and thawing on mechanical properties of Qinghai–Tibet clay. Cold Regions Science and Technology 48:34–43.

Weaver, K. N., S. E. Alfano, A. R. Kronquist, and D. M. Reeder. 2009. Healing rates of wing punch wounds in free-ranging little brown myotis (*Myotis lucifugus*). Acta Chiropterologica 11:220–223.

Wheeler, J. B., R. Mukherjee, R. E. Stroud, J. A. Jones, and J. S. Ikonomidis. 2015. Relation of murine thoracic aortic structural and cellular changes with aging to passive and active mechanical properties. Journal of the American Heart Association 4:e001744.

Woods, M., R. A. McDonald, and S. Harris. 2003. Predation of wildlife by domestic cats *Felis catus* in Great Britain. Mammal Review 33:174–188.

Submitted 20 December 2018. Accepted 17 April 2019.

Associate Editor was John Scheibe.